

## Dirac Coupled Channel Analyses of Proton Scatterings from $^{54}\text{Fe}$ Nucleus

Sugie Shim\*

Physics Department, Kongju National University, Gongju, Republic of Korea

**Abstract:** Relativistic coupled channel analysis based on the Dirac equation is performed for the inelastic scatterings of 800 MeV polarized proton from the  $^{54}\text{Fe}$  nucleus using an optical potential model and a rotational collective model. Employing the Dirac phenomenology, the optical potential parameters and deformation parameters are varied to reproduce the experimental data. The theoretical results are observed to agree reasonably well with the inelastic scattering experimental data, showing a little better agreement with the data than those obtained in the nonrelativistic calculations. The channel coupling effect for the excited states those belong to the ground state rotational band at the deformed nucleus is also investigated. The effective Schroedinger equivalent central and spin-orbit potentials are calculated by reducing the Dirac equation to the Schroedinger-like second order differential equation and analyzed. Surface-peaked phenomena are observed at the imaginary effective central potentials and the effective spin-orbit potentials.

**Keywords:** Proton inelastic scattering, Dirac coupled channel analyses, Collective model, Optical potential model

### 1. INTRODUCTION

Relativistic approaches based on the Dirac equation as the relevant wave equation have been remarkably successful in treating nuclear structure and nuclear reactions [1-6]. We have worked on Dirac coupled channel analyses of proton inelastic scatterings from spherically symmetric nuclei and several deformed nuclei successfully [7-11] and observed that the multistep processes via channel couplings are important for the intermediate energy proton inelastic scatterings from the deformed nuclei. However, it is still necessary to expand Dirac coupled channel analysis to intermediate energy scatterings from various deformed nuclei in order to have systematic analyses of relativistic calculations.

In this work we use optical potential model [5, 6] in Dirac coupled channel calculation to analyze 800 MeV proton inelastic scattering from  $^{54}\text{Fe}$  nucleus, for which

the relativistic Dirac analysis has not been reported so far. We use phenomenological optical potentials, employing S-V model [6, 7] where only scalar and time-like vector potentials are considered. In order to obtain the transition optical potentials a first order rotational collective model is used to describe the collective motion of the excited deformed nucleus considering the low lying excited states of the ground state rotational band (GSRB) [8]. Because multistep processes must be carefully included for proper description of proton-nucleus inelastic scattering for the deformed nuclei [12, 13], the multistep process is included in the calculation by considering the channel coupling between two excited states. By fitting the elastic and inelastic scattering data for  $p+^{54}\text{Fe}$ , Dirac optical potential and deformation parameters are determined using a computer program called ECIS [14], which employs the sequential iteration method. The Dirac equations are reduced to the Schroedinger-like second-order differential equations and the effective central and spin-orbit optical potentials obtained and analyzed. The calculated deformation parameters for the low-lying excited states of the ground state rotational band in the nucleus are compared with those obtained in the nonrelativistic calculations.

### 2. THEORY AND RESULTS

Relativistic analysis of 800 MeV proton inelastic scattering from the  $^{54}\text{Fe}$  nucleus is performed using an optical potential model and the collective model in the Dirac coupled channel formalism. The Dirac equation for the nucleon-nucleus elastic scattering is given as

$$[\alpha \cdot p + \beta(m + U_S) - (E - U_V^0 - V_C) + i\alpha \cdot \hat{r}\beta U_T]\Psi(r) = 0.$$

Here,  $U_S$  is a scalar potential,  $U_V^0$  is a time-like vector potential,  $U_T$  is a tensor potential, and  $V_C$  is the Coulomb potential. For the even-even nuclei (spin-0) [4], only scalar, time-like vector and tensor optical potentials survive as in the spherically symmetric nuclei [7]. The scalar and the time-like vector potentials are used as direct potentials in the calculation. Even though tensor potentials are always present due to the interaction of

the anomalous magnetic moment of the projectile with the charge distribution of the target, they have been found to be always very small compared to scalar or vector potentials [8]. Hence they are neglected in this calculation. The scalar and vector optical potentials are given as

$$U_s = V_s f_s(r) + iW_s g_s(r)$$

$$U_V^0 = V_V^0 f_V(r) + iW_V^0 g_V(r),$$

where  $V_s$  and  $W_s$  are the strengths of the real and imaginary scalar potential,  $V_V^0$  and  $W_V^0$  are the strengths of real and imaginary time-like vector potential, respectively. We assume that these potentials have Fermi distribution as they are assumed to follow the distribution of nuclear density. Fermi model form factors of the Woods-Saxon shape for the Dirac optical potentials are given as

$$f_i(r), g_i(r) = \frac{1}{1 + \exp\left[\frac{r - R_{0,i}}{Z_i}\right]},$$

where  $R_{0,i}$  and  $Z_i$  are potential radius and diffusiveness, respectively and the subscript  $i$  stands for the real and imaginary scalar, and the real and imaginary vector potentials. Even though Lorentz scalar, time-like vector and tensor potentials survive for elastic scattering when spin-zero targets are considered, depending on the model assumed, pseudo-scalar and axial-vector potentials may also be present in the case of inelastic scattering. In the collective model approach used in this work we assume that we can obtain appropriate transition potentials by deforming the direct potentials that describe the elastic channel reasonably well [7]. Assuming the shape of the deformed potentials follows the shape of deformed nuclear densities, the transition potentials are obtained by setting to be proportional to the first derivatives of the diagonal potentials, as in Tassi model. The first order transition potentials are given by

$$U_i^\lambda(r) = \frac{\beta_i^\lambda R_i}{(2\lambda + 1)^{1/2}} \frac{dU_i(r)}{dR_i} Y_{\lambda 0}^*(\Omega),$$

with  $\lambda$  being the multipolarity,  $\beta$  a deformation parameter, and  $R$  the radius parameter of the Woods-Saxon shape. We consider both couplings between the  $0^+$  ground state and the low lying excited states and also coupling between two adjacent excited states, for example, between the  $2^+$  and  $4^+$  states. Hence the multistep process is included in the calculation. Because the channel coupling between the excited states of GSRB can be strong in the inelastic scattering

from a deformed nucleus, the multistep transition process could be important. Dirac coupled channel calculations are done in which the phenomenological direct potential strengths are varied along with the deformation parameters. The Dirac coupled channel equations are solved numerically to calculate the experimental observables using the computer code ECIS [14] which employs the sequential iteration method. The Schroedinger-like second order Dirac equation is calculated by considering the upper component of the Dirac wave function, and the effective central and spin-orbit optical potentials are obtained [7, 11] to be compared with the results obtained using those of the Schroedinger calculations.

The experimental data for the differential cross sections and analyzing powers are obtained from [15, 16] for the 800 MeV polarized proton elastic and inelastic scatterings from the deformed nucleus,  $^{54}\text{Fe}$ . The low lying excited states of GSRB ( $K=0^+$ ),  $2^+$  (1.408 MeV) and  $4^+$  (2.538 MeV) states are considered and assumed to be collective rotational states in the calculation. Firstly, 12 parameters of the diagonal scalar and vector potentials in the Woods-Saxon shapes are phenomenologically searched to reproduce the experimental elastic scattering data. The Dirac equations are solved to obtain the best fitting optical potential parameters to the experimental data by using the minimum chi-square ( $\chi^2$ ) method. The 12 Woods-Saxon potential parameters obtained by fitting the elastic scattering data are given in **Table 1**. The real scalar potentials and the imaginary vector potentials turn out to be large and negative, and that the imaginary scalar potentials and the real vector potentials turn out to be large and positive, showing the same pattern as in the spherically symmetric nuclei [5, 9].

**Table 1:** The optical potential parameters of Woods-Saxon shape obtained in the relativistic Dirac phenomenological calculations for the 800 MeV polarized proton elastic scatterings from  $^{54}\text{Fe}$  nucleus.

Potential	Strength (MeV)	Radius (fm)	Diffusiveness (fm)
Scalar real	-311.0	3.725	0.763
Scalar imaginary	146.5	2.656	0.791
Vector real	172.3	3.760	0.736
Vector imaginary	-118.7	3.675	0.611

Next, all of the optical potential-parameters and deformation parameters are searched by including the lowest-lying excited state of the ground state rotational band, the  $2^+$  state (1.408 MeV), in addition to the ground state in the calculation, starting from the 12 parameters for the direct optical potentials obtained in the elastic scattering calculation. In most of our previous works, we searched for the two deformation parameters,  $\beta_s$  and  $\beta_v$ , per each excited state by assuming the real and imaginary deformation parameters are the same [7-11]. However, we set  $\beta_s$  and  $\beta_v$  are the same in this work and searched for only one deformation parameter,  $\beta_2$ , in order to have the same number of parameters with those in the nonrelativistic calculations. Finally, we included all three states of the GSRB,  $0^+$ ,  $2^+$ , and  $4^+$  states, in the calculation in order to see the multistep effect. The optical potential parameters obtained by fitting the elastic scattering data in the elastic scattering calculation are varied because the channel coupling of the excited states to the ground state should be included in the inelastic scattering calculation.

The results of the coupled channel calculations for the ground state are shown in the **Figure 1** and it is shown that relativistic Dirac coupled channel calculation using an optical potential model could describe the ground state for 800 MeV polarized proton inelastic scatterings from the  $^{54}\text{Fe}$  nucleus very well. In figures, "cpd" means "coupled" and the blue lines are the results obtained from the nonrelativistic calculations. It is shown that the results of relativistic and nonrelativistic calculations give almost same quality fits to the experimental data for the ground state. We use the same computer program ECIS [14] for the nonrelativistic calculations. The results of the coupled channel calculations for the  $2^+$  excited state in the ground state rotational band are shown in the **Figure 2** and it is shown that relativistic Dirac coupled channel calculation using an optical potential model could describe the low-lying  $2^+$  excited states of the ground state rotational band for 800 MeV polarized proton inelastic scatterings from the  $^{54}\text{Fe}$  nucleus pretty well, showing that the theoretical results of the Dirac calculations reproduce the experimental data slightly better than those of nonrelativistic calculations, especially for the spin analyzing power ( $A_y$ ) data. It is shown that the agreements with data are not changed significantly by adding  $4^+$  state in the calculation, showing that the channel coupling effect of the multistep process does not play important role for the

low lying state excitations of the GRSB at the proton inelastic scattering from  $^{54}\text{Fe}$  nucleus.

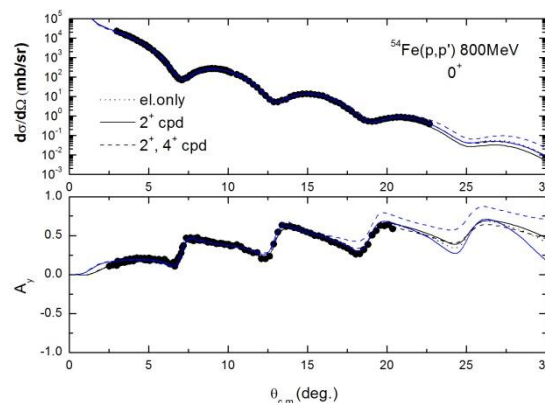


**Figure 1:** Comparison of the results of Dirac coupled channel calculations with the ground state experimental data of 800 MeV polarized proton inelastic scatterings from  $^{54}\text{Fe}$  nucleus and those of nonrelativistic calculations.

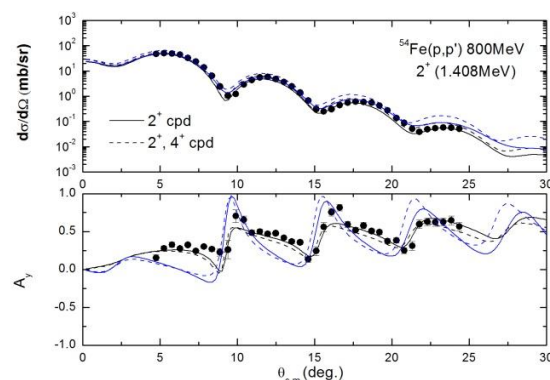


**Figure 2:** Comparison of the results of Dirac coupled channel calculations with the  $2^+$  state experimental data of 800 MeV polarized proton inelastic scatterings from  $^{54}\text{Fe}$  nucleus and those of nonrelativistic calculations.

In **Figure 3**, the results of the coupled channel calculations for the  $4^+$  excited state in the ground state rotational band are shown and both relativistic and nonrelativistic calculation could not describe the experimental data very well, missing the minimum points of the data, even though the results of the relativistic calculation could reproduce the data slightly better than those of nonrelativistic calculations.

In **Table 2 and 3**, we show the optical potential parameters of the Woods-Saxon shape and the deformation parameters for the  $2^+$  and  $4^+$  excited states of the  $^{54}\text{Fe}$  nucleus obtained in the relativistic Dirac coupled channel calculations and those obtained in the nonrelativistic coupled channel calculations.

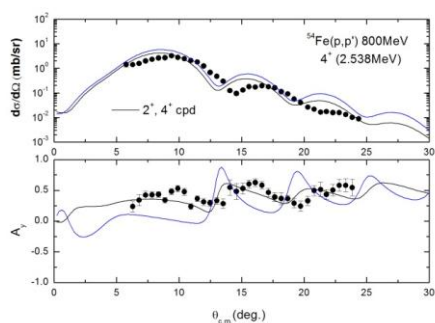


**Figure 3:** Comparison of the results of Dirac coupled channel calculations with the  $4^+$  state experimental data of 800 MeV polarized proton inelastic scatterings from  $^{54}\text{Fe}$  nucleus and those of nonrelativistic calculations.

**Table 2:** The optical potential parameters of Woods-Saxon shape and the deformation parameters obtained in the relativistic Dirac coupled channel calculations for the 800 MeV proton inelastic scatterings from  $^{54}\text{Fe}$  nucleus.

Potential	Strength (MeV)	Radius (fm)	Diffusiveness (fm)	$\beta_2$	$\beta_4$
Scalar real	-373.8	3.525	0.796	0.171	0.079
Scalar imaginary	167.3	2.769	0.733		
Vector real	203.4	3.616	0.757		
Vector imaginary	-125.1	3.678	0.593		

**Table 3:** The optical potential parameters of Woods-Saxon shape and the deformation parameters obtained in the nonrelativistic coupled channel calculations for the 800 MeV proton inelastic scatterings from  $^{54}\text{Fe}$  nucleus.

Potential	Strength (MeV)	Radius (fm)	Diffusiveness (fm)	$\beta_2$	$\beta_4$
Central real	-4.048	4.313	0.216	0.197	0.097
Central imaginary	67.23	3.919	0.510		
Spin-orbit real	0.729	3.779	0.641		
Spin-orbit imaginary	1.714	3.780	0.604		

It is observed that the deformation parameters obtained in the Dirac phenomenological coupled channel calculation for the  $2^+$  and  $4^+$  state excitations of the  $^{54}\text{Fe}$  nucleus show quite good agreement with those obtained in the nonrelativistic calculations using the same Woods-Saxon potential shape for the geometries of the optical potentials.

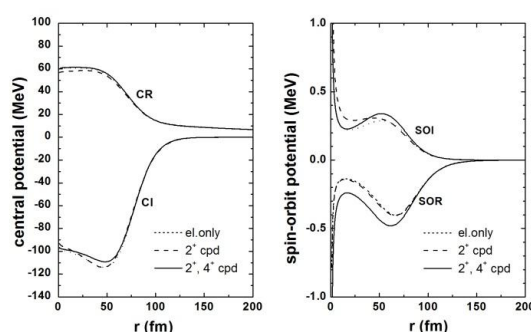


**Figure 4:** The effective central and spin-orbit potentials of  $^{54}\text{Fe}$  nucleus. CR and CI represent central real and imaginary potentials, and SOR and SOI represent spin-orbit real and imaginary optical potentials, respectively.

In **Figure 4**, we show the effective central and spin-orbit potentials of the  $^{54}\text{Fe}$  nucleus. We show the effective potentials for the cases of elastic calculation (dotted line), where the ground and  $2^+$  states are coupled (dashed line), and where all three states are coupled (solid line). Surface-peaked phenomena are clearly observed for the imaginary parts of the effective central potentials (CI) for the scattering from  $^{54}\text{Fe}$ , while the surface-peaked phenomena are not clearly observed for the real parts of the central potentials (CR), for all three cases. The surface-peaked phenomena are clearly shown at the effective spin-orbit potentials, and the effective spin-orbit potential strengths turned out to be about the same order with those obtained from nonrelativistic calculations, as shown in **Table 3**, even though the sign is the opposite for the real spin-orbit potential. It should be noted that one of the merits of the relativistic approach based on the Dirac equation instead of using the nonrelativistic approach based on the Schrodinger equation is that the spin-orbit potential appears naturally in the Dirac approach when the Dirac equation is reduced to a Schrodinger-like second-order differential equation, while the spin-orbit potential should be inserted by hand in the conventional nonrelativistic Schrodinger approach.

### 3. CONCLUSIONS

Relativistic Dirac coupled channel analyses are performed for the 800MeV polarized proton inelastic scatterings from  $^{54}\text{Fe}$  nucleus using an optical potential model. The optical potential parameters are obtained phenomenologically using the scalar-vector potential model. It is shown that the theoretical results of the relativistic Dirac calculations reproduce the

experimental data very well, showing a little better agreements with the data than those obtained in the nonrelativistic calculations, especially for the spin analyzing power ( $A_y$ ) data. The channel coupling effect of the multistep process turns out to be not significant for the low lying state excitations of the GRSB at the proton inelastic scattering from  $^{54}\text{Fe}$  nucleus. By reducing Dirac equations to the Schroedinger-like second-order differential equations, the effective central and spin-orbit potentials are obtained and the surface-peaked phenomena are observed at the imaginary effective central potentials for the scattering from  $^{54}\text{Fe}$  nucleus. The first-order rotational collective models are used to describe the low-lying excited states of the ground state rotational bands in the  $^{54}\text{Fe}$  nucleus, and the obtained deformation parameters are found to agree pretty well with those of the nonrelativistic calculations using the same Woods-Saxon potential shape.

#### ACKNOWLEDGEMENT

This work was supported by Basic Science Research Program through the National Research Foundation of Korea (NRF) funded by the Ministry of Education (2016R1D1A1B01014355).

#### REFERENCES

- [1] L. S. Celenza and C. M. Shakin, "Relativistic nuclear physics", World Scientific, New-York, 1986.
- [2] M. R. Anastasio, L. S. Celenza, W. S. Pong, and C. M. Shakin, "Relativistic nuclear structure physics", Physics Reports, vol. 100, pp. 327-401, 1983.
- [3] C. J. Horowitz and B. D. Serot, "Self-consistent hartree description of finite nuclei in a relativistic quantum field theory", Nucl. Phys. A vol. 368, pp. 503-528, 1981.
- [4] R. J. Furnstahl, C. E. Price, and G. E. Walker, "Systematics of light deformed nuclei in relativistic mean-field models", Phys. Rev. C vol. 36, pp. 2590-2600, 1987.
- [5] L. G. Arnold, B. C. Clark, R. L. Mercer, and P. Swandt, "Dirac optical model analysis of  $p - ^{40}\text{Ca}$  elastic scattering at 180 MeV and the wine-bottle-bottom shape", Phys. Rev. C, Vol. 23, pp. 1949-1959, 1981
- [6] J. A. McNeil, J. Shepard, and S. J. Wallace, "Impulse-approximation Dirac optical potential", Phys. Rev. Lett, vol. 50, pp. 1439-1442, 1983.
- [7] S. Shim, "Relativistic analyses of nucleon-nucleus inelastic scatterings", Ph.D. Thesis, The Ohio State University, U. S. A., 1989.
- [8] S. Shim, B. C. Clark, E. D. Cooper, S. Hama, R. L. Mercer, L. Ray, J. Raynal, and H. S. Sherif, "Comparison of relativistic and nonrelativistic approaches to the collective model treatment of  $p+^{40}\text{Ca}$  inelastic scattering", Phys. Rev. C, vol. 42, pp. 1592-1597, 1990.
- [9] S. Shim, B. C. Clark, E. D. Cooper, S. Hama, R. L. Mercer, L. Ray, J. Raynal, and H. S. Sherif, "Comparison of relativistic and nonrelativistic approaches to the collective model treatment of  $p+^{40}\text{Ca}$  inelastic scattering", Phys. Rev. C, Vol. 42, pp. 1592-1597, 1990.
- [10] S. Shim, M. W. Kim, B. C. Clark, and L. Kurth Kerr, "Dirac coupled channel analyses of 800 MeV proton inelastic scattering from  $^{24}\text{Mg}$ ", Phys. Rev. C, Vol. 59, No. 1, pp. 317-322, 1999.
- [11] S. Shim and M. W. Kim, "Systematic Dirac Analyses of Proton Inelastic Scatterings from Axially Symmetric Deformed Nuclei", Int. Jou. of Mod. Phys. E, Vol. 21, No. 12, pp. 1250098.1-1250098.10, 2012.
- [12] M. L. Barlett, J. A. McGill, L. Ray, M. M. Barlett, G. W. Hoffmann, N. M. Hintz, G. S. Kyle, M. A. Franey, and G. Blanpied, "Proton scattering from  $^{154}\text{Sm}$  and  $^{176}\text{Yb}$  at 0.8 GeV", Phys. Rev. C, vol. 22, pp. 1168-1179, 1980.
- [13] S. Shim, and M. W. Kim, "Relativistic analysis of proton inelastic scattering from an axially symmetric deformed nucleus", Sae Mulli, vol. 40, pp. 545-553, 2000.
- [14] J. Raynal, "Computing as a language of physics", ICTP International Seminar Course, 281, IAEA, Italy, 1972; J. Raynal, Notes on ECIS94, Note CEA-N-2772, 1994.
- [15] L. Ray and G. W. Hoffmann, "Proton isotonic density differences from 0.8 GeV proton - nucleus elastic scattering", Phys. Rev. C, Vol. 27, pp. 2143-2149, 1983.
- [16] G. S. Adams, Th. S. Bauer, t G. Igo, G. Pauletta, C. A. Whitten, Jr., and A. Wriekat, G. W. Hoffmann, G. R. Smith, M. Gazzaly, "800-MeV inelastic proton scattering from  $^{40}\text{Ca}$ ,  $^{48}\text{Ca}$ , and  $^{54}\text{Fe}$ ", Phys. Rev. C, Vol. 21, pp. 2485-2495, 1983.